Research Square

Preprints are preliminary reports that have not undergone peer review.
They should not be considered conclusive, used to inform clinical practice,
or referenced by the media as validated information.

A Time-Dependent Creep Constitutive Model of Deep Surrounding Rock Under Temperature-Stress Coupling

Xiaofeng Li (m15036032451@163.com)
Liaoning Technical University
Zhixiang Yin
Liaoning Technical University

Original Paper

Keywords: Creep, Nishihara model, variable parameters, accelerated creep, timeliness

Posted Date: February 2nd, 2021

DOI: https://doi.org/10.21203/rs.3.rs-162852/v1

License: This work is licensed under a Creative Commons Attribution 4.0 International License.
Read Full License

A time-dependent creep constitutive model of deep surrounding rock under temperature-stress coupling

Xiaofeng Li • Zhixiang Yin

Abstract: In order to study the creep behavior of surrounding rock of Hengda coal mine in Fuxin under different temperature, the triaxial creep test of sandstone is carried out by MTS815.02 test system. Based on the Nishihara model, the model creep parameters are denormalized by introducing the relationship among damage variables, time and temperature. The improved variable parameter creep aging model is obtained. The creep parameters are identified by least squares method. The correctness of the creep model is verified by comparing the experimental data with the model curves. The results show that the instantaneous strain to the total strain ratio decreases first and then increases due to the compaction deformation of the internal voids under the initial stress level. The decrease of temperature effectively increases the rock bearing capacity and delays the creep damage time. The established variable-time aging creep model can not only describe the rock attenuation creep and stable creep deformation characteristics, but also makes up for the shortcomings of the traditional creep model that can not describe the accelerated creep characteristics. And it predict the development law of creep deformation well. The model is in good agreement with the test curve, which shows the correctness and rationality of the model. It has guiding significance for actual engineering support and prediction of long-term deformation of surrounding rock.

Key words: Creep; Nishihara model; variable parameters; accelerated creep; timeliness

1 Introduction

After the deep coal mining, the surrounding rock of the roadway undergoes time-dependent deformation under the action of the supporting body, and this time-related deformation is generally called rheology (Anno et al.1998). For the study of rheological properties of rock under external loads, a rheological model describing rheological properties is established, which has practical guiding significance for predicting surrounding rock deformation and design support scheme (Tao et al.2013). As the mining depth increases, the mechanical properties of rock are no longer the linear variation law when the shallow part is present, and the rock mechanical properties show nonlinear variation characteristics (Jia et al.2018). Not only soft rock produces rheology, but hard rock (such as sandstone, marble and granite) has obvious rheological properties (Shlyannikov et al.2018). In order to further study the creep deformation characteristics and creep deformation failure mechanism of rock under high confining pressure, high temperature, high ground stress and strong disturbance condition, it is necessary to carry out indoor creep test on rock. Furthermore, a suitable creep constitutive model can be constructed by experimental conditions and data, which is of great significance for studying the creep mechanism of materials (Zhou et al.2012;Winkel et al.1972).

In recent years, scholars had done a lot of research on the rheological properties of rocks, the mechanism of deformation and failure, and how to construct a suitable creep model (Wang et al.2017;Xiong et al.2017). The establishment of the model includes the following methods:(1) A nonlinear nonlinear creep model was constructed by the series-parallel connection of basic components and the nonlinearization of components; (2)The rock damage creep constitutive model was constructed by combining thermodynamic theory and damage mechanics theory; (3)Through a large number of experimental research results, the empirical creep model formula was summarized and the model parameter determination method was proposed; (4)A fractional-order creep constitutive model was established by transforming the integer-order component model into a fractional-order

X . Li (First author and Corresponding Author)
Liaoning Technical University, Fuxin 123000 China;E-mail: m15036032451@163.com)
Z . Yin
Liaoning Technical University, Fuxin 123000 China;E-mail: 3121570334@qq.com)

component model. Based on the multi-load creep test of sandstone with different initial damage levels, a new nonlinear nonlinear creep damage model was proposed. The model not only described three typical creep stages, but also shown the effect of initial damage on creep failure stress (Hou et al.2018). Wang et al.(2015) constructed a micro-mechanical damage-friction coupling model, and applied the model to the triaxial compression test and triaxial creep test of simulated granite. The numerical data could be used to predict the experimental data well. The fractional differential element was used to replace the viscous element in the traditional Nishihara model, and the nonlinear creep parameter creep model of rock was established (Li et al.2018). The shear creep behavior of the key unit rock of the potential sliding surface of the landslide was studied by shear creep test. A new plastic nonlinear model (PFY model) was proposed to characterize the progressive failure creep characteristics reflected in the limiting shear creep process of rock (Zhang et al.2019). Hadiseh Mansouri et al.(2018) conducted axial compression tests and triaxial creep tests on salt rock in salt wells in southern Iran. The mechanical properties of rocks were studied and a nonlinear creep model of rock was constructed.

Although the model in the above study can describe the acceleration of creep deformation of the rock into the cerebral blood vessels, the creep equation was finally formed to had a low degree of fitting for accelerated creep deformation. Therefore, it was very important to choose a simple transformation of creep parameters into time-dependent functions, and then derived nonlinear creep equations. In this paper, the creep deformation characteristics of the surrounding rock of the roadway in Hengda Coal Mine of Liaoning Province under different temperature were analyzed. The Nishihara model creep parameters were all converted into time-dependent functions. The rheological theory was used to recalculate the relationship between temperature and stress and time. A time-dependent creep constitutive model of deep surrounding rock under temperature-stress coupling was constructed. Finally, the correctness of the creep model was verified by comparing the experimental data with the model curve.

2 Establishment of time-dependent model

2.1 Establishment of variable parameter model in one-dimensional state

The Nishihara model consists of an elastomer, a viscoelastic body and a viscoplastic body(Qi et al.2012). The one-dimensional model expression for the Nishihara model is as follows(Yao et al.2018; Zhao et al.2017).

When $\sigma<\sigma_s$,

$$\varepsilon = \frac{\sigma}{E_0} + \frac{\sigma}{E_1}\left[1 - \exp\left(-\frac{E_1}{\eta_1}t\right)\right] \tag{1a}$$

When $\sigma \geqslant \sigma_s$,

$$\varepsilon = \frac{\sigma}{E_0} + \frac{\sigma}{E_1}\left[1 - \exp\left(-\frac{E_1}{\eta_1}t\right)\right] + \frac{\sigma - \sigma_s}{\eta_2}t \tag{1b}$$

where σ is the stress, E_0 is the elastic modulus of the elastomer, E_1 is the elastic modulus of the viscoelastic body, η_1 is the viscosity coefficient of the viscoelastic body, η_2 is the viscosity coefficient of the viscoplastic body, and σs is the yield stress.

The mechanical properties of roadway surrounding rock in complex deep geological environment can not be explained by conventional mechanics theory. At this time, the mechanical properties and creep properties of surrounding rock has obvious nonlinear characteristics. In order to describe this nonlinear creep deformation characteristic, the creep parameter can no longer be used as a fixed value. It is a function of time variation. The creep parameter and time relationship function can be expressed as

$$Z = Z(t) \tag{2}$$

where Z is a variable representing all creep parameters.

It is assumed that the variation law of damage variable and time product satisfis (Desayi et al.1995)

$$D = 1 - \exp\left[-\left(\frac{t}{\alpha} \right)^{m} \right] \tag{3}$$

where α is the parameter that characterizes the internal damage of the rock, m is the non-uniformity of damage distribution of meso-probability voxels.

It is assumed that the non-uniform distribution parameter m inside the rock is connected with the fracture network. Generally, the room temperature is 25 ℃. The relationship between the non-uniformity coefficient m and the temperature is

$$m = a(T-25)^2 + b(T-25) + c \tag{4}$$

where a,b and c are coefficients related to temperature.

The relationship between damage variable and temperature and time is obtained by combining equations (3) and (4).

$$D = 1 - \exp\left[-\left(\frac{t}{\alpha} \right)^{a(T-25)^2 + b(T-25) + c} \right] \tag{5}$$

It can be defined that the rock creep parameter Z has the following relationship with the damage variable D .

$$Z(D,\ t) = Z(1-D) \tag{6}$$

The equation (5) is substituted into equation (6). The relationship between rock creep parameters and time is obtained as

$$Z(D,\ t) = Z \cdot \exp\left[-\left(\frac{t}{\alpha} \right)^{a(T-25)^2 + b(T-25) + c} \right] \tag{7}$$

The total strain ε satisfies the equation (9) under one-dimensional stress(Yao et al.2018).

$$\varepsilon = \varepsilon_e + \varepsilon_{ve} + \varepsilon_{vp} \tag{8}$$

where ε_e is the elastic strain, ε_{ve} is the viscoelastic strain, ε_{vp} is the viscoplastic strain.

The change law of elastic modulus is only related to stress. Therefore, the damage variable of elastic modulus satisfies(Singh et al.2018).

$$E_0(D,\ t) = E_0 \exp\left[-\left(\frac{t}{\alpha_0} \right)^{a_0(T-25)^2 + b_0(T-25) + c_0} \right] \tag{9}$$

where α_0 is the damage influence factor related to stress;a_0,b_0 and c_0 are coefficients related to temperature.

The elastic strain of the rock is not affected by time, but it is affected by the stress. In the one-dimensional state, the elastic strain ε_e of the rock satisfis the equation (10).

$$\varepsilon_e = \frac{\sigma}{E_0 \exp\left[-\left(\frac{t}{\alpha_0} \right)^{a_0(T-25)^2 + b_0(T-25) + c_0} \right]} \tag{10}$$

In the one-dimensional state, the viscoelastic strain ε_{ve} of the rock satisfis the equation (11).

$$\sigma = E_1 \exp\left[-\left(\frac{t}{\alpha_1} \right)^{a_1(T-25)^2+b_1(T-25)+c_1} \right] \varepsilon_{ve} + \eta_1 \exp\left[-\left(\frac{t}{\alpha_2} \right)^{a_2(T-25)^2+b_2(T-25)+c_2} \right] \varepsilon'_{ve} \tag{11}$$

where α_1 and α_2 is the time coefficient of influence of the viscoelastic body; a_1,b_1, c_1,a_2,b_2 and c_2 are coefficients related to temperature.

In order to facilitate the calculation, it is assumed that the spring of the viscoelastic body is consistent with the degree of damage to the viscous pot. That is, $\alpha_1=\alpha_2$, $a_1=a_2$,$b_1=b_2$ and $c_1=c_2$.

The integral solution of equation (11) is used to obtain the viscoelastic strain expression.

$$\varepsilon_{ve} = \left\{ \int \frac{\sigma}{\eta_1} \exp\left[\left(\frac{t}{\alpha_1} \right)^{a_1(T-25)^2+b_1(T-25)+c_1} + \frac{E_1}{\eta_1} t \right] + C_0 \right\} \exp\left(-\frac{E_1}{\eta_1} t \right) \tag{12}$$

where C_0 is the integral constant.

Since the exponential function cannot be integrated, the Taylor series is used to expand the exponential function.

$$\exp\left[\left(\frac{t}{\alpha_1} \right)^{a_1(T-25)^2+b_1(T-25)+c_1} + \frac{E_1}{\eta_1} t \right] = 1 + \left(\frac{t}{\alpha_1} \right)^{a_1(T-25)^2+b_1(T-25)+c_1} + \frac{E_1}{\eta_1} t + o\left(t^2\right) \tag{13}$$

By integrating equation (13), equation (14) can be obtained.

$$t + \frac{\alpha_1}{a_1(T-25)^2 + b_1(T-25) + c_1 + 1} \left(\frac{t}{\alpha_1} \right)^{a_1(T-25)^2+b_1(T-25)+c_1+1} + \frac{E_1}{2\eta_1} t^2 + C_0 \tag{14}$$

The initial conditions are: t=0 and ε_{ve}=0. The viscoelastic deformation is

$$\varepsilon_{ve} = \frac{\sigma}{\eta_1} \left\{ t + \frac{\alpha_1}{a_1(T-25)^2 + b_1(T-25) + c_1 + 1} \left(\frac{t}{\alpha_1} \right)^{a_1(T-25)^2+b_1(T-25)+c_1+1} + \frac{E_1}{2\eta_1} t^2 \right\} \exp\left(-\frac{E_1}{\eta_1} t \right) \tag{15}$$

In the one-dimensional state, the viscoelastic strain εvp of the rock satisfis the equation (16).

$$\sigma = \begin{cases} \eta_2 \exp\left[-\left(\dfrac{t}{\alpha_2} \right)^{a_3(T-25)^2+b_3(T-25)+c_3} \right] \dot{\varepsilon}_{vp}, & \sigma < \sigma_s \\ 0, & \sigma < \sigma_s \end{cases} \tag{16}$$

where α_2 is the time influence coefficient of the viscoplastic body; a_3,b_3 and c_3 are coefficients related to temperature.

The exponential function is expanded by using Taylor series.The integral solution of equation (16) is solved to obtain a viscoplastic strain expression.

$$\varepsilon_{vp} = \frac{\sigma}{\eta_2} \left[t + \frac{\alpha_1}{a_1(T-25)^2 + b_1(T-25) + c_1 + 1} \left(\frac{t}{\alpha_1} \right)^{a_3(T-25)^2+b_3(T-25)+c_3+1} \right] \tag{17}$$

2.2 Establishment of variable parameter model in three-dimensional state

In the actual project, the surrounding rock of the roadway is in a three-direction stress state, and the above

model can not describe the multi-directional force creep characteristics. This requirs transforming the one-dimensional model into a three-dimensional model (Cyr et al.2015;Yang et al.2015).

However, the total strain ε_{ij} of the Nishihara model in the three-direction stress state satisfis the equation (18).

$$\varepsilon_{11} = \varepsilon_{11}^{e} + \varepsilon_{11}^{ve} + \varepsilon_{11}^{vp} \tag{18}$$

where ε^{e}_{11} is the elastic strain in the three-dimensional state, ε^{ve}_{11} is the viscoelastic strain in the three-dimensional state; ε^{vp}_{11} is the viscoplastic strain in the three-dimensional state.

The elastic strain in the three-dimensional state is not affected by time, but it is affected by the stress state. The elastic strain can be expressed as a function of the stress state by the elastic model in the one-dimensional state.

$$\varepsilon_{11}^{e} = \frac{\sigma_1 + 2\sigma_3}{9K\exp\left[-\left(\frac{t}{\alpha_0}\right)^{a_0(T-25)^2+b_0(T-25)+c_0}\right]} + \frac{\sigma_1 - \sigma_3}{3G_0\exp\left[-\left(\frac{t}{\alpha_0}\right)^{a_0(T-25)^2+b_0(T-25)+c_0}\right]} \tag{19}$$

where K is the bulk modulus, G_0 is the elastomer shear modulus.

The expression of viscoelastic strain affected by time in three-dimensional state is

$$\varepsilon_{\mathrm{ve}} = \frac{\sigma_1 - \sigma_3}{3\eta_1}\left\{t + \frac{\alpha_1}{a_1(T-25)^2 + b_1(T-25) + c_1 + 1}\left(\frac{t}{\alpha_1}\right)^{a_1(T-25)^2+b_1(T-25)+c_1+1} + \frac{G_1}{2\eta_1}t^2\right\}\exp\left(-\frac{G_1}{\eta_1}t\right) \tag{20}$$

The viscoplastic strain in the three-dimensional state can not be directly convert by analogy. It is also affected by the plastic potential function and the yield function. Therefore, the viscoplastic strain in the three-dimensional state can be expressed as

$$\varepsilon_{11}^{vp} = \frac{F}{\eta_2\exp\left[-\left(\frac{t}{\alpha_2}\right)^{a_3(T-25)^2+b_3(T-25)+c_3}\right]}\frac{\partial F}{\partial \sigma_{11}}t \tag{21}$$

In general, the yield function selects the generalized Drucker Prage yield function.

$$F = \sqrt{J_2} - \xi I_1 - k = (\sigma_1 - \sigma_3)/\sqrt{3} - \xi(\sigma_1 + 2\sigma_3) - k\,, \tag{22}$$

where I_1 is the first invariant of stress; J_2 is the second invariant of stress bias, ξ and k is the test parameter.

The test parameters ξ and k are functions of internal friction angle and cohesion.

$$\xi = \frac{\sin\varphi}{\sqrt{3}\sqrt{3+\sin^2\varphi}};\quad k = \frac{\sqrt{3}C\cos\varphi}{\sqrt{3+\sin^2\varphi}} \tag{23}$$

where φ is the angle of internal friction; C is the cohesion.

The internal friction angle and cohesion will also deteriorate under the action of time and temperature.

$$\xi(T,t) = \frac{\sin\varphi\exp\left[-\left(\frac{t}{\alpha_2}\right)^{a_3(T-25)^2+b_3(T-25)+c_3}\right]}{\sqrt{3}\sqrt{3+\sin^2\varphi\exp\left[-\left(\frac{t}{\alpha_2}\right)^{a_3(T-25)^2+b_3(T-25)+c_3}\right]}} \tag{24}$$

$$k(T,t)=\frac{\sqrt{3}C\exp\left[-\left(\frac{t}{\alpha_2}\right)^{a_3(T-25)^2+b_3(T-25)+c_3}\right]\cos\varphi\exp\left[-\left(\frac{t}{\alpha_2}\right)^{a_3(T-25)^2+b_3(T-25)+c_3}\right]}{\sqrt{3+\sin^2\varphi\exp\left[-\left(\frac{t}{\alpha_2}\right)^{a_3(T-25)^2+b_3(T-25)+c_3}\right]}} \tag{25}$$

Therefore, the viscoplastic strain of the rock can be obtained as

$$\varepsilon_{11}^{vp}=\frac{\left[\frac{1}{\sqrt{3}}-\xi\cdot(T,t)\right]}{\eta_2\exp\left[-\left(\frac{t}{\alpha_2}\right)^{a_3(T-25)^2+b_3(T-25)+c_3}\right]}\left\{\frac{(\sigma_1-\sigma_3)}{\sqrt{3}}-\xi(T,t)(\sigma_1+2\sigma_3)-k(T,t)\right\}t \tag{26}$$

The time-dependent constitutive equation for obtaining rock in three-dimensional state is

When $\sigma<\sigma_s$,

$$\varepsilon=\frac{\sigma_1+2\sigma_3}{9K\exp\left[-\left(\frac{t}{\alpha_0}\right)^{a_0(T-25)^2+b_0(T-25)+c_0}\right]}+\frac{\sigma_1-\sigma_3}{3G_0\exp\left[-\left(\frac{t}{\alpha_0}\right)^{a_0(T-25)^2+b_0(T-25)+c_0}\right]}+\frac{\sigma_1-\sigma_3}{3\eta_1}\cdot$$
$$\left\{t+\frac{\alpha_1}{a_1(T-25)^2+b_1(T-25)+c_1+1}\left(\frac{t}{\alpha_1}\right)^{a_1(T-25)^2+b_1(T-25)+c_1+1}+\frac{G_1}{2\eta_1}t^2\right\}\exp\left(-\frac{G_1}{\eta_1}t\right) \tag{27}$$

When $\sigma\geqslant\sigma_s$ and $\varepsilon<\varepsilon_a$,

$$\varepsilon=\frac{\sigma_1+2\sigma_3}{9K\exp\left[-\left(\frac{t}{\alpha_0}\right)^{a_0(T-25)^2+b_0(T-25)+c_0}\right]}+\frac{\sigma_1-\sigma_3}{3G_0\exp\left[-\left(\frac{t}{\alpha_0}\right)^{a_0(T-25)^2+b_0(T-25)+c_0}\right]}+\frac{\sigma_1-\sigma_3}{3\eta_1}\cdot$$
$$\left\{t+\frac{\alpha_1}{a_1(T-25)^2+b_1(T-25)+c_1+1}\left(\frac{t}{\alpha_1}\right)^{a_1(T-25)^2+b_1(T-25)+c_1+1}+\frac{G_1}{2\eta_1}t^2\right\}\exp\left(-\frac{G_1}{\eta_1}t\right) \tag{28}$$
$$+\frac{\left[\frac{1}{\sqrt{3}}-\xi\cdot(T,t)\right]}{\eta_2\exp\left[-\left(\frac{t}{\alpha_2}\right)^{a_3(T-25)^2+b_3(T-25)+c_3}\right]}\left\{\frac{(\sigma_1-\sigma_3)}{\sqrt{3}}-\xi(T,t)(\sigma_1+2\sigma_3)-k(T,t)\right\}t$$

3 Creep test

3.1 Creep test plan

In this paper, the surrounding rock (sandstone) of the roadway in Hengda Coal Mine of Fuxin is shown in Fig. 1. According to the requirements of the International Rock Mechanics Society for standard test pieces, the surrounding rock was made into a cylindrical sample with a height of 100 mm and a diameter of 50 mm.It must be ensured that the non-parallelism and unevenness of both ends of the specimen are less than 0.05mm. Prior to the

test, Vaseline was evenly applied to both end faces of the rock to eliminate the end effect during the test. The test equipment used the MTS815.02 rock test system (shown in Fig. 2). Its maximum confining pressure was 100MPa, and the precise range of force measurement was -1%~+1%, which met the requirements of this test.



Fig. 1 Part of the samples

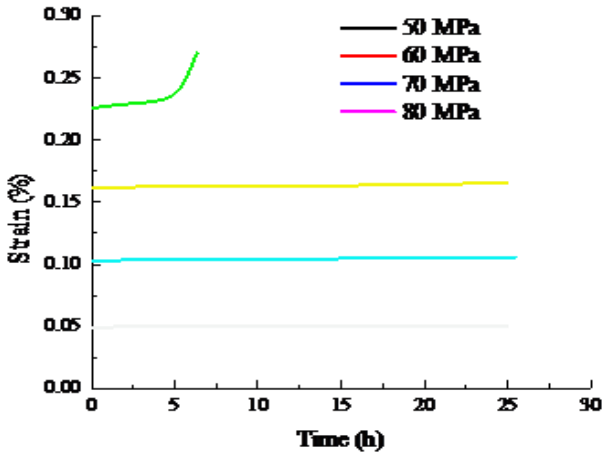


Fig. 2 MTS815.02 rock three triaxial test machine

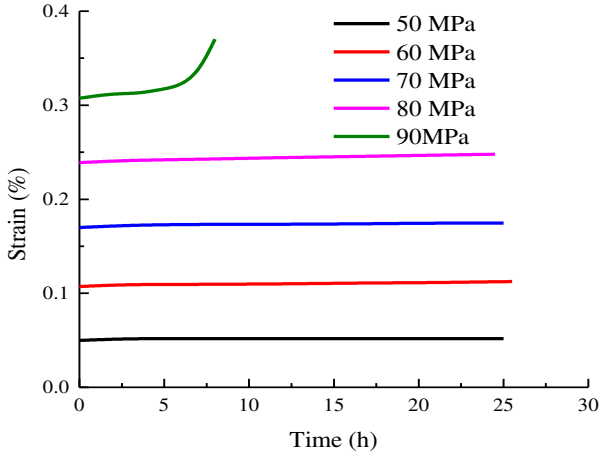
In this paper, the indoor triaxial creep test was carried out by the single specimen gradual loading method. First, the confining pressure was applied to a predetermined value, and the confining pressure was selected to be 10 MPa. The temperature of the creep test is set to 100 and 200°C. The stress levels were 50, 60, 70 and 80 MPa. After the confining pressure was stabilized, the axial pressure wa applied. The applied load rate was set to 500 N/s. The temperature is loaded to the predetermined temperature at a rate of 0.5°C/s.When applying axial stress, it must be ensured that the confining pressure had been changed within a controllable range of the predetermined value. After the stress level creep deformation entered the stable creep, the next level of load application began. This cycle was repeated until the rock sample was destroyed. Finally, the test data was saved at intervals of 3 s. After unloading the confining pressure and the axial pressure, the sample is taken out and stored.

3.2 Analysis of creep characteristics

The single test piece is gradually loaded to complete the creep test, and the creep data under each load is affected by the historical load. Therefore, the data need to be processed by the Chen's superposition method. The axial creep deformation-time curve of the surrounding rock of the roadway under different temperature is shown in Fig. 3.



(a)T=200℃



(b)T=100℃

Fig. 3 Axial creep duration curve

It can be seen from Fig. 3 that the creep deformation curves of rock under different temperature are basically the same. Under the action of temperature of 200℃, the failure deformation failure occurs after the fourth stage of load. Under the action of temperature of 100℃, the failure deformation failure occurs after the fifth stage of load. The instantaneous strain and creep strain increased with the increase of stress level, and the ratio of instantaneous strain to total strain first decreases and then increases. This is due to the compaction of the internal voids of the rock under the initial stress level. Taking the temperature of 200 ℃ as an example, under the action of low stress (50 MPa), the rock deformation has only transient strain and decay creep deformation. Finally, the rock creep deformation rate decays to zero. Under medium stress (60 and 70 MPa), rock creep has two kinds of attenuation creep and stable creep. At this time, the creep rate does not decay to zero, but decays to a stable value and enteres the stage of creep to be stabilized. The creep deformation of the rock keeps this creep rate continuously deformed. Under high stress (80MPa), the rock appeares to accelerate creep deformation. After the first two creep stages, the rock enteres the accelerated creep stage. The creep rate accumulation increases, and finally the internal crack of the rock penetrats to form a fracture surface. The last creep time of the rock decreases with the increase of temperature. When the temperature is 200℃, the last stage creep time is 6.32h, and the final stage creep time is 7.89h when the confining pressure is 100℃. This show that the decrease of temperature effectively increases the rock bearing capacity and increases the creep damage time.

4 Verification of creep aging constitutive model

Before verifying the rock creep aging model, the long-term strength of the rock under different confining pressures need to be determined (Kravcov et al.2017). The long-term strength of the rock can be determined by

isochronous stress-strain curves. The isochronous stress-strain curve under the action of temperature of 200℃ is shown in Fig. 4.

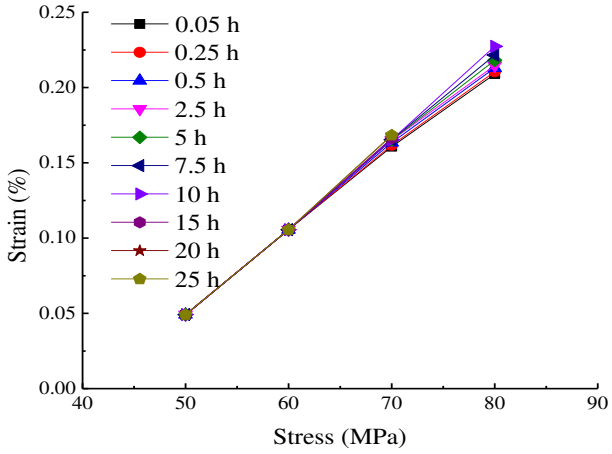


Fig. 4 Isochronic stress-strain curve

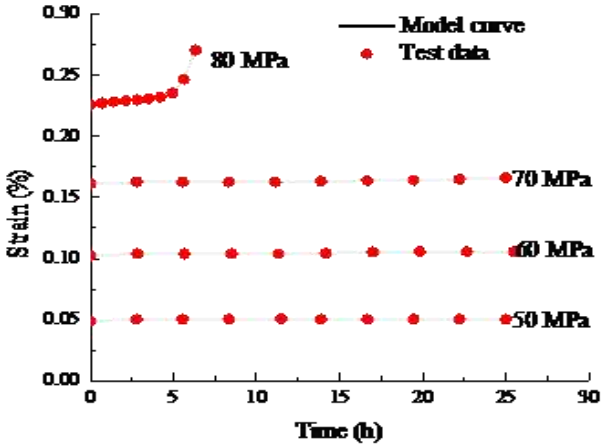
It can be seen from Fig. 4 that the isochronous stress-strain curve of the rock is a cluster of divergent broken line segments. The rock stress and strain show a linear change before the divergence point. After the divergence point, the rock stress and strain basically show nonlinear linear variation. Therefore, the divergence point corresponding stress value can be used as the long-term strength value of the rock. Under the action of temperature of 200℃, the long-term strength of the rock is 60MPa.

The improved creep model was fitted by least squares method, and the creep parameters are obtained as shown in Table 1(taking 200℃ as an example) .

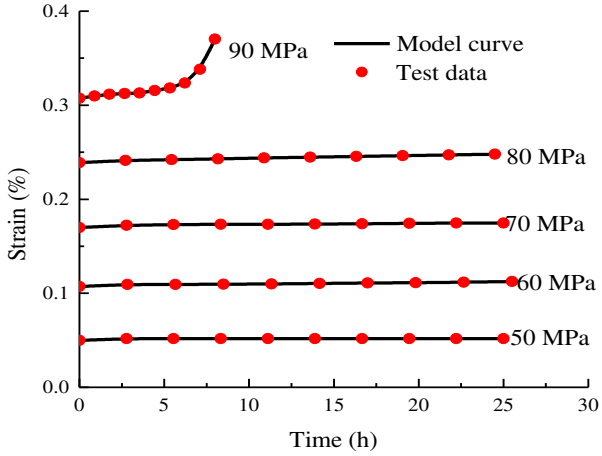
Tab. 1 Fitting values of creep parameters

σ_1/MPa	50	60	70	80
G_0/GPa	8.71	8.53	7.77	7.45
K/GPa	7.29	7.13	6.50	5.23
G_1/GPa	13.15	12.88	11.73	11.24
η_1/(GPa·h)	927.58	1198.17	1441.43	1994.14
η_2/(GPa·h)	-	9973.61	12251.13	16569.11
α_0	1.46	1.22	0.93	0.75
α_1	2.07	2.03	1.82	1.72
α_2	-	0.46	0.50	0.75
a_0	0.03	0.07	0.12	0.23
$a_1(a_2)$	0.11	0.24	0.32	0.46
a_3	0.52	0.57	0.65	0.78
b_0	0.91	1.02	1.18	1.47
$b_1(b_2)$	0.38	0.41	0.58	0.84
b_3	-	0.89	0.95	1.09
c_0	0.41	0.56	0.89	1.40
$c_1(c_2)$	1.42	1.66	1.96	2.29
c_3	-	0.89	1.34	1.92
R^2	0.975	0.987	0.951	0.923

Substituting parameters of different stress levels into the model, the model curves of the rock under different stress levels are obtained. The comparison between the model curve and the experimental data is shown in Fig. 5(a). In the same way, the model curve and test curve of rock under the temperature of 100℃ can be obtained as shown in Fig. 5(b).



(a)T=200℃



(b)T=100℃

Fig.5 Comparison curves

It can be seen from Fig. 5 that the rock model curve and the experimental data has a good fitness, and the correlation coefficients are all above 0.90. It is shown that the variable parameter time-dependent creep model established in this paper can not only describe the rock attenuation creep and stable creep deformation characteristics, but also this model makes up for the shortcomings of the traditional creep model which can not describe the accelerated creep characteristics. And it is a good predictor of the development of creep deformation. At the same time, the model is in good agreement with the experimental curve, which indicats the correctness and rationality of the model. It has guiding significance for actual engineering support and prediction of long-term deformation of surrounding rock.

5 Conclusion

In this paper, the creep behavior of the surrounding rock of Hengda Coal Mine in Fuxin under different temperature is analyzed. The creep parameters of the Nishihara model is transformed into time-dependent functions. Furthermore, A time-dependent creep constitutive model of deep surrounding rock under temperature-stress coupling is constructed.

The instantaneous strain and creep strain increases with the increase of stress level, and the ratio of instantaneous strain to total strain first decreases and then increases. This is due to the compaction of the internal voids of the rock under the initial stress level.

The rock model curve and the experimental data had a good fitness, and the correlation coefficients are all above 0.90. It is shown that the variable parameter time-dependent creep model established in this paper can not only describe the rock attenuation creep and stable creep deformation characteristics, but also this model makes up for the shortcomings of the traditional creep model which can not describe the accelerated creep

characteristics.

It is a good predictor of the development of creep deformation. The model is in good agreement with the experimental curve, which indicats the correctness and rationality of the model. It has guiding significance for actual engineering support and prediction of long-term deformation of surrounding rock.

Acknowledgments

We gratefully acknowledged the National Natural Science Foundation of China (51774173) for funding this work.

Data availability statement

The data used to support the findings of this study are available from the corresponding author upon request.

Compliance with Ethical Standards

The authors declare no conflict of interest.

References

Anno (1998) Time-dependent Behaviour of Deep Level Tabular Excavations in Hard Rock. Rock Mechanics and Rock Engineering, 32(2):123-155.

Tao M , Li X , Li D (2013) Rock failure induced by dynamic unloading under 3D stress state.Theoretical and Applied Fracture Mechanics,65(6):47-54.

Jia S P, Zhang L W, Wu B S (2018) A coupled hydro-mechanical creep damage model for clayey rock and its application to nuclear waste repository. Tunnelling and Underground Space Technology, 74:230-246.

Shlyannikov V, Tumanov A (2018) Creep damage and stress intensity factor assessment for plane multi-axial and three-dimensional problems. International Journal of Solids & Structures, 15:166-183.

Zhou CB, Wan ZJ, Zhang Y (2012) Creep characteristics and constitutive model of gas coal mass under high temperature and triaxial stress. Journal of China Coal Society, 12:2020-2025.

Winkel BV, Gerstle KH, Ko HY (1972) Analysis of time-dependent deformations of openings in salt media." International Journal of Rock Mechanics and Mining Sciences, 9(2):249-260.

Wang R, Zhuo Z, Zhou H W (2017) A fractal derivative constitutive model for three stages in granite creep. Results in Physics,7:2632-2638.

Xiong Y L, Ye G L, Zhu H H (2017) A unified thermo-elasto-viscoplastic model for soft rock." International Journal of Rock Mechanics and Mining Sciences, 93(3):1-12.

Hou R, Zhang K, Tao J (2018) A Nonlinear Creep Damage Coupled Model for Rock Considering the Effect of Initial Damage.Rock Mechanics and Rock Engineering,(2):1-11.

Wang W , Liu H X , Zhu Q Z(2015) A micromechanics-based creep damage model for brittle rocks. European Journal of Environmental and Civil Engineering,19(S1):s1-s14.

Li Z D (2018) Nonlinear Variation Parameters Creep Model of Rock and Parametric Inversion. Geotechnical and Geological Engineering,36(5):2985-2993.

Zhang H,Zhao H B,Zhang X Y (2019) Creep Characteristics and Model of Key Unit Rock in Slope Potential Slip Surface. International Journal of Geomechanics,19(8):.935-944.

Hadiseh M , Rassoul A (2018) Mechanical behavior of salt rock under uniaxial compression and creep tests. International Journal of Rock Mechanics and Mining Sciences, 110:19-27.

Qi YJ, Jiang QH, Wang ZJ (2012) 3D creep constitutive equation of modified Nishihara model and its parameters identification. Chinese Journal of Rock Mechanics and Engineering, 31(2): 347-355.

Yao XL, Qi JL, Zhang JM (2018) A one-dimensional creep model for frozen soils taking temperature as an independent variable.Soils and Foundations,58(6):627-640.

Zhao Y, Wang Y, Wang W (2017) Modeling of non-linear rheological behavior of hard rock using triaxial rheological experiment. International Journal of Rock Mechanics and Mining Sciences,93(3):66-75.

Desayi P, Nandakumar N (1995) A semi-empirical approach to Predict shear strength of ferrocement. Cement and Concrete Composite,17(3):207-218.

Yao X, Qi J, Zhang J (2018) A one-dimensional creep model for frozen soils taking temperature as an independent variable. Soils & Foundations, S0038080618300374.

Singh A, Kumar C, Kannan L G (2018) Estimation of creep parameters of rock salt from uniaxial compression tests[J]. International Journal of Rock Mechanics & Mining Sciences, 107:243-248.

Cyr E D , Mohammadi M , Mishra R K (2015) A three dimensional (3D) thermo-elasto-viscoplastic constitutive model for FCC polycrystals. International Journal of Plasticity,70:166-190.

Yang S Q, Xu P, Xu T (2015) Nonlinear visco-elastic and accelerating creep model for coal under conventional triaxial compression.Geomechanics and Geophysics for Geo-Energy and Geo-Resources, (1):109-120.

Kravcov, Alexander N, Svoboda P, Pospíchal V (2017) Assessment of Long-Term Strength of Rocks. Key Engineering Materials, 755:62-64.

Figures



Figure 1

Part of the samples



Figure 2

MTS815.02 rock three triaxial test machine

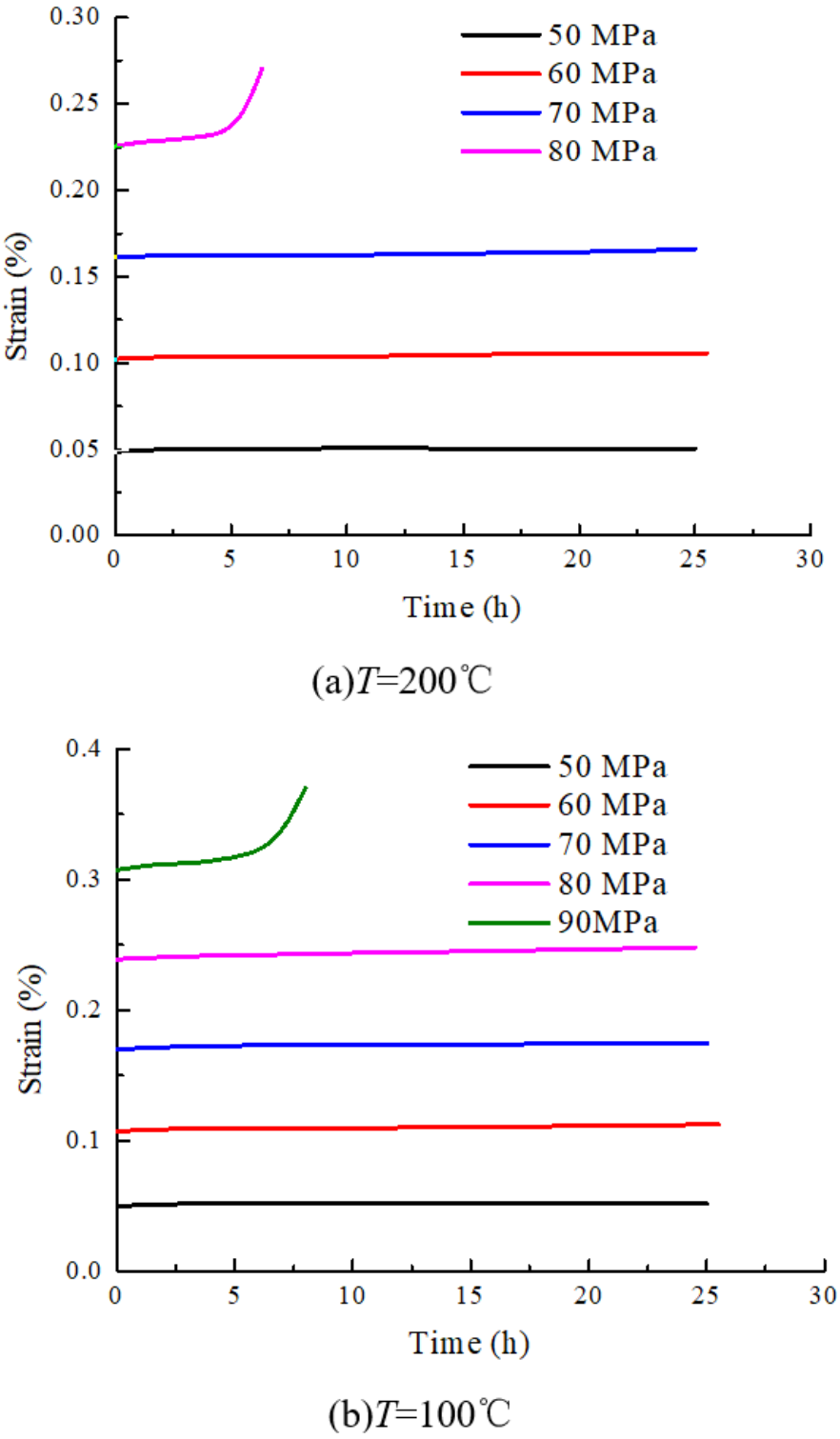


Figure 3

Axial creep duration curve

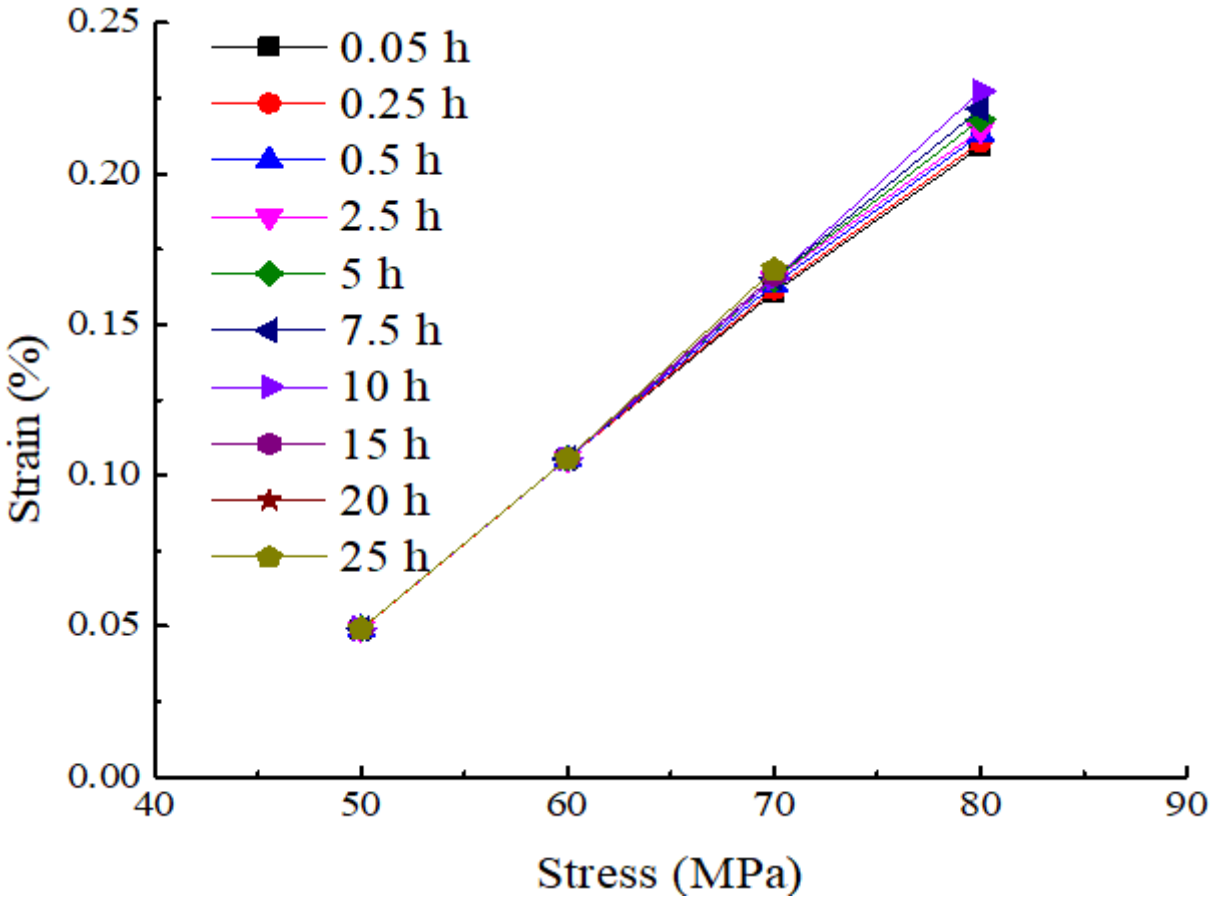


Figure 4

Isochronic stress-strain curve

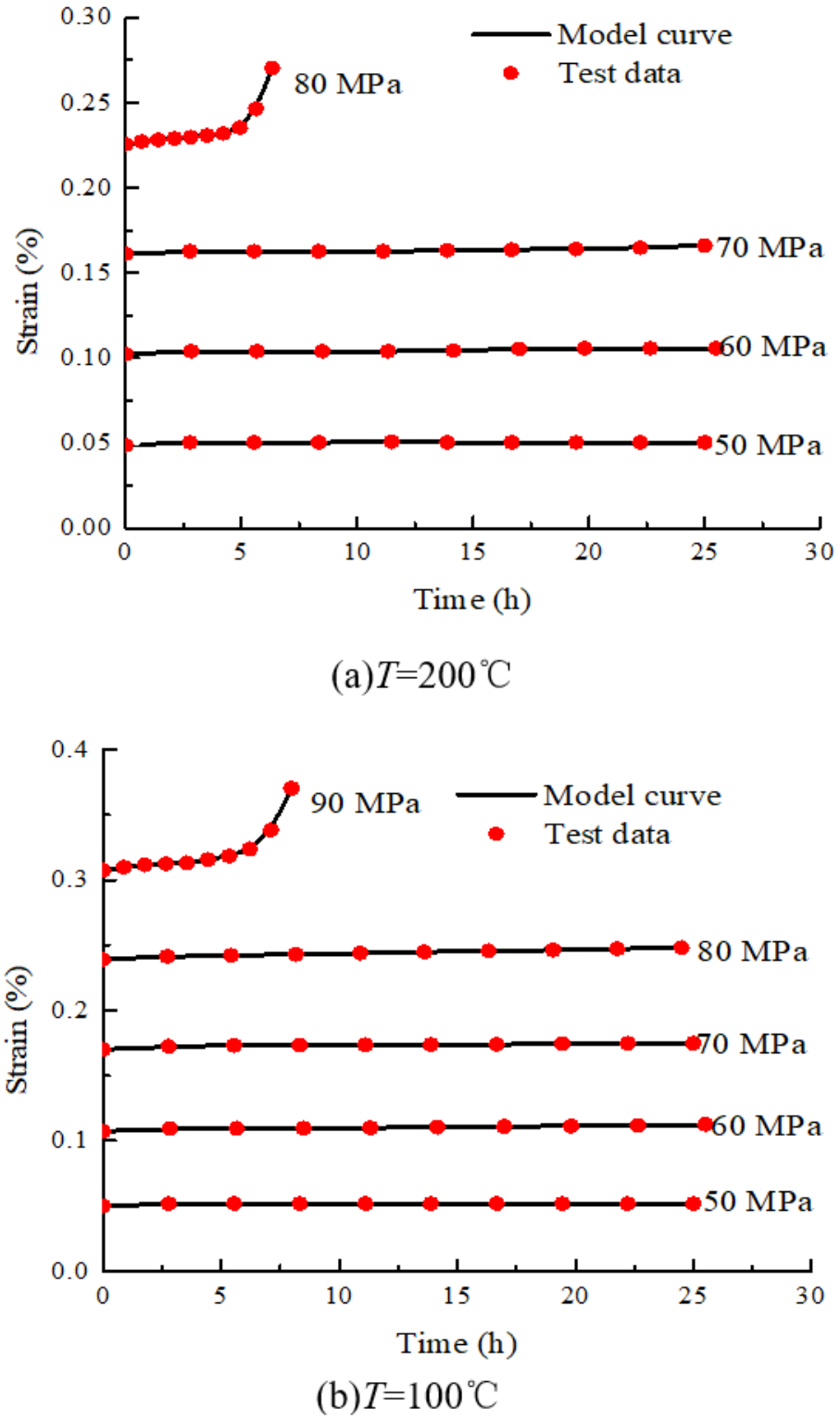


Figure 5

Comparison curves